Heliyon 10 (2024) e28664

Contents lists available at ScienceDirect

Heliyon

journal homepage: www.cell.com/heliyon

Research article

Discovering common pathogenetic processes between tuberculosis and COVID-19 by bioinformatics and system biology approach

Xin Liu [1], Haoran Li [1], Yilin Wang [1], Shanshan Li, Weicong Ren, Jinfeng Yuan [**], Yu Pang [*]

Department of Bacteriology and Immunology, Beijing Chest Hospital, Capital Medical University/Beijing Tuberculosis and Thoracic Tumor Research Institute, Beijing, China

ARTICLE INFO

Keywords:
SARS-CoV-2
Tuberculosis
Common gene
TF regulatory network
Drug molecule

ABSTRACT

Background: SARS-CoV-2, the cause of the COVID-19 pandemic, poses a significant threat to humanity. Individuals with pulmonary tuberculosis (PTB) are at increased risk of developing severe COVID-19, due to long-term lung damage that heightens their susceptibility to full-blown disease.

Methods: Three COVID-19 datasets (GSE157103, GSE166253, and GSE171110) and one PTB dataset (GSE83456) were obtained from the Gene Expression Omnibus databases. Subsequently, data were subjected to weighted gene co-expression network analysis(WGCNA)followed by functional enrichment analysis using Gene Ontology (GO) and Kyoto Encyclopedia of Genes and Genomes (KEGG) pathway databases. These analyses revealed two overlapping disease-specific modules, each comprising co-regulated genes with potentially related biological functions. Using Cytoscape, we visualised the interaction network containing common disease-related genes found within the intersection between modules and predicted transcription factors (TFs). Real-time qPCR was conducted to quantify expression levels of these genes in blood samples from COVID-19 and PTB patients. Finally, DisGeNET and the Drug Signatures database were employed to analyze these common genes, unveiling their connections to clinical disease features and potential drug treatments.

Results: Examination of the overlap between COVID-19 and PTB gene modules unveiled 11 common genes. Functional enrichment analyses using KEGG and GO shed light on potential functional relationships among these genes, providing insights into their potential roles in the heightened mortality of PTB patients due to SARS-CoV-2 infection. Furthermore, results of various bioinformatics-based analyses of common TFs and target genes led to identification of shared pathways and therapeutic targets for PTB patients with COVID-19, along with potential drug treatments for these patients.

Conclusion: Our results unveiled a potential biological connection between COVID-19 and PTB, as supported by results of functional enrichment analysis that highlighted potential biological processes and signaling pathways shared by both diseases. Building on these findings, we propose potential drug treatments for PTB patients with COVID-19, pending verification of drug safety and efficacy through laboratory and multicentre studies before clinical use.

* Corresponding author.
** Corresponding author.
E-mail addresses: yuanjinfeng0920@163.com (J. Yuan), pangyupound@163.com (Y. Pang).
[1] These authors contributed equally to this work.

https://doi.org/10.1016/j.heliyon.2024.e28664
Received 1 August 2023; Received in revised form 20 March 2024; Accepted 21 March 2024
Available online 27 March 2024

1. Introduction

Mycobacterium tuberculosis (Mtb), the causative agent of tuberculosis (TB), has plagued humanity for centuries and remains a significant global threat despite extensive efforts to curb its transmission [1]. TB is highly contagious and is transmitted through aerosol dispersion. The clinical manifestations of *Mtb* infection vary greatly and are strongly influenced by the host immune response [2]. Individuals with weakened immune systems, such as those with HIV or undergoing immunosuppressive therapy, face an elevated risk of contracting TB [3].

Mtb primarily targets the lungs but can disseminate to other organs, including the brain, meninges, lymph nodes, bones, and joints, leading to extrapulmonary TB. Uncontrolled *Mtb* infection can result in multiorgan failure and death [4]. In response to the global TB challenge, the World Health Organisation (WHO) introduced the End TB Strategy with the objective of achieving a 90% reduction in TB incidence by 2035.

While substantial efforts have been directed towards eliminating TB, the emergence of the COVID-19 pandemic has posed new challenges to global health systems and communities worldwide, significantly impacting progress toward meeting the 2035 End TB Strategy goal. According to the *WHO Global Tuberculosis 2023 Report*, a total of 771,407,825 confirmed COVID-19 cases and 6,972,152 deaths from this disease have been reported worldwide [5].

Clinical manifestations of COVID-19 range from mild flu-like symptoms to severe respiratory failure [6]. A growing body of evidence indicates that severe COVID results from SARS-CoV-2 disruption of the host immune system, potentially leading to serious complications related to viral triggering of cytokine storm and multiorgan damage, especially of the heart and kidneys [7,8]. Meanwhile, COVID-19 patients co-infected with bacterial pathogens, such as *Staphylococcus aureus*, *Mycoplasma pneumoniae*, *Legionella pneumophila*, *Klebsiella pneumoniae*, and *Acinetobacter baumannii*, reportedly have elevated morbidity and mortality rates [9]. Furthermore, co-infections with these pathogens can exacerbate clinical COVID-19 symptoms, leading to severe forms of pneumonia, prolonged ICU stays, and complicated treatments [10].

In high-TB burden countries, the elevated prevalence of patients afflicted with both COVID-19 and TB has raised concerns regarding overlapping clinical symptoms, potential drug interactions, and increased complication rates after TB treatment completion [11]. Both COVID-19 and TB are airborne respiratory diseases that disrupt pulmonary immune regulation, posing a dual risk of exacerbating COVID-19 severity and promoting TB disease progression. Moreover, co-infected individuals have been reported to possess reduced numbers of *Mtb*-specific $CD4^+$ T cells, leading to high mortality rates [12]. However, few research studies have focused on the pathogenic mechanisms underlying co-infection susceptibility. To bridge this knowledge gap, here we employ bioinformatics-based approaches to identify shared key genes between COVID-19 and PTB as potential targets for interventional therapies for use in treating patients afflicted with both diseases.

2. Method

2.1. Data collection and processing

The study flowchart is outlined in Fig. 1. Three COVID-19 datasets (GSE157103, GSE166253, and GSE171110) and one PTB dataset

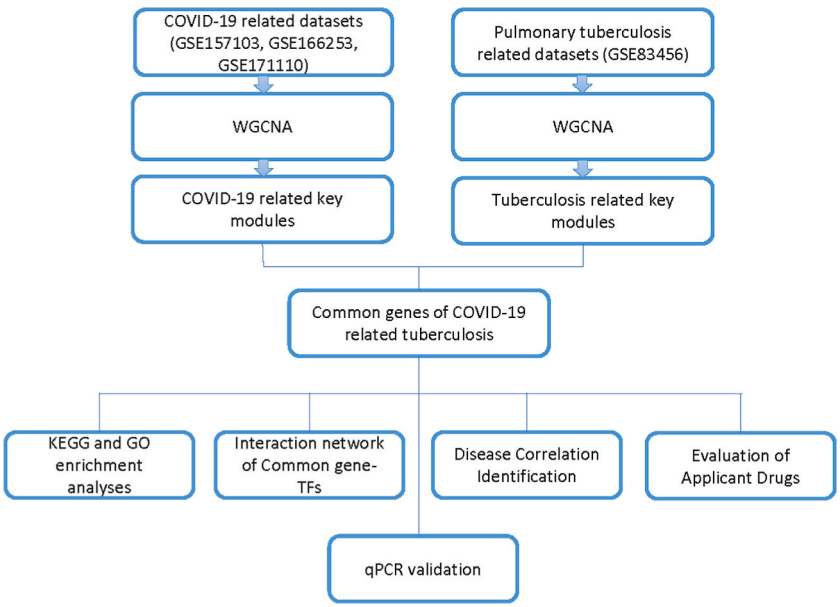

Fig. 1. Flow diagram of the entire process: data collection, processing, analysis, and validation.

(GSE83456) were retrieved from the Gene Expression Omnibus public database collection. To mitigate batch effects inherent in all samples, we employed surrogate variable analysis (SVA, version 3.14) in conjunction with principal component analysis (PCA). Following data preprocessing and probe annotation, we extracted common genes from separate COVID-19 and PTB datasets. This process resulted in the creation of two new gene expression matrices, each representing all samples.

Construction of a network based on weighted gene co-expression network analysis (WGCNA) results for use in identifying COVID-19/PTB-related gene modules.

The 'WGCNA' R package was employed to construct a WGCNA network with the aim of identifying co-expressed gene modules based on the set of common genes obtained in the aforementioned analysis. The network was built using a weighted adjacency matrix employing the power function, with power values (β) for soft thresholds derived through the "pickSoftThreshold" algorithm. To achieve a scale-free network β values of 18 for COVID19-WGCNA and 5 for TB-WGCNA were selected as appropriate soft thresholds. Subsequently, the adjacency matrix was converted into a topological overlap matrix (TOM) to enhance network stability and reliability.

Utilizing TOM-based dissimilarity measures, we employed the mean linked age-stratified clustering technique to organize genes with comparable expression patterns into modules. A gene dendrogram was created with a minimum group size of 30 genes. Module significance and correlation were assessed using Spearman correlation analysis and hierarchical clustering. Modules related to COVID-19 or PTB were considered significant if their P-values were below 0.05 and their correlation coefficient (r) values exceeded 0.3. An examination of genes within the intersection of both modules enabled the identification of a set of common genes associated with both diseases.

Gene ontology (GO) and Kyoto Encyclopedia of Genes and Genomes (KEGG) pathway enrichment analysis of genes related to both COVID-19 and PTB.

GO analyses were conducted to identify functional terms within the categories of biological process (BP), cellular component (CC), and molecular function (MF). The results were visualised using the online DAVID 6.7 tool (https://david-d.ncifcrf.gov/), offering valuable insights into the biological significance of common genes associated with both COVID-19 and PTB. Additionally, KEGG pathway enrichment analysis was performed with clusterProfiler, applying a significance threshold of $P < 0.05$ to the results obtained from both GO and KEGG analyses.

2.2. Construction of a regulatory network composed of transcription factors and common genes

ChIP-Atlas, an integrated data mining tool used to process open-source ChIP-seq data, was employed to identify potential regulatory interactions between predicted TFs and identified common hub genes. The resulting regulatory network comprised of TFs and common genes was then visualised using Cytoscape software to gain a comprehensive understanding of the intricate regulatory relationships among these components.

2.3. Identification of candidate drugs

We utilized the Drug Signatures database (DSigDB), which contains 22,527 gene expression profiles of cells or tissues exposed to drugs or other stimuli, to identify drug molecules with potential efficacy against both COVID-19 and PTB. The DSigDB database, which is accessible through the Enrichr platform (https://amp.pharm.mssm.edu/Enrichr/), is an enrichment analysis tool that provides comprehensive graphical information on collective functions of a set of input genes.

2.4. The DisGeNET resource

We employed DisGeNET[13], a comprehensive database of human gene-disease connections, to gather separate summaries of all gene-disease and variant-disease associations. Thorough searches of DisGeNET for genes associated with COVID-19 and/or TB diseases yielded summaries featuring original metrics, including scores for gene-disease associations, disease specificity, and pleiotropy indexes. Our primary objective was to identify robust gene-disease associations with scores below 0.3, indicating strong links between genotype and phenotype.

2.5. Patients and ethics

Blood samples were collected from ten COVID-19 and ten TB patients, each of whom provided written informed consent. The study received approval from the Ethics Committee (Approval Number: YJS-2022-03) and adhered to the guidelines outlined in the Declaration of Helsinki.

2.6. Real-time quantitative PCR (qPCR)

Total RNA was purified from blood samples using TRIzol (Invitrogen), followed by reverse transcription of 1 μg of RNA into complementary DNA using the High-Capacity RNA-to-cDNA Kit (Applied Biosystems). The resulting cDNA was then subjected to real-time quantitative PCR (qPCR) analysis using an ABI 7500 Real-Time PCR System (Applied Biosystems). Real-time qPCR results are presented as the mean ± standard deviation (SD) from three independent experiments, each conducted in duplicate. Group comparisons were performed using Student's t-test or one-way ANOVA with Bonferroni's correction as appropriate. Statistical significance

was indicated by P-values below 0.05.

3. Results

3.1. Construction of the weighted gene co-expression network and identification of core modules

After background correction and expression normalization, COVID-19 expression matrices generated from GSE157103, GSE166253, and GSE171110 datasets and PTB expression matrices generated from the GSE83456 dataset collectively formed our training dataset. Surrogate variable analysis (SVA) was then conducted to eliminate batch effects, as confirmed by PCA plots (Fig. 2A and B).

Subsequently, we performed WGCNA on the training dataset to identify highly correlated gene expression patterns associated with COVID-19 or PTB disease status. An essential step in WGCNA is the selection of an optimal soft threshold (β) that balances network sparsity and achieves a scale-free topology. Typically, β values range from 1 to 30 or higher. The scale-free topology fit index, typically evaluated using the R^2 fit, is computed for each β value. This process aims to identify the specific β value at which the R^2 fit either plateaus or reaches its peak, all while preserving a scale-free network structure. In this study, we chose a β of 18 for COVID19-WGCNA and a β of 5 for PTB-WGCNA. These values provided the desired balance for constructing meaningful co-expression networks, as illustrated in Fig. 3A, Fig. S1A, Fig. 4A, and Fig. S1B.

Genes with similar expression patterns were organized into gene modules, as depicted in Figs. 3B and 4B. We identified 17 gene modules associated with COVID-19 (Fig. 3C) and 14 gene modules related to PTB (Fig. 4C). Analysis of module eigengenes (MEs) and module significance (MS) values revealed that the blue module exhibited the highest correlation with COVID-19 (Fig. 3D), while the yellow module had the strongest association with PTB (Fig. 4D). These results indicated that the blue module was most closely linked to COVID-19, while the yellow module had the strongest relationship with PTB. Finally, common genes between the two diseases were obtained by examining the intersection of COVID-19-related and TB-related modules.

3.2. Functional enrichment analysis of key genes related to both COVID-19 and TB

To uncover biological themes related to common genes, we employed GO analysis using the DAVID database with the threshold for the false discovery rate (FDR) of <0.05 and the threshold for gene limit of ≥ 10. Results of GO analysis of common genes revealed enrichment of MF terms *phosphatidylinositol 3-kinase binding*, *phosphatidylinositol phosphate phosphatase activity*, and *SNAP receptor activity* (SNAP stands for soluble NSF attachment protein; NSF stands for N-ethylmaleimide sensitive factor), CC terms *tertiary granule membrane*, *specific granule membrane*, and *synaptic vesicle membrane*, and the BP term *RNA splicing* (Fig. 5A, Table 3). Additionally, KEGG enrichment analysis revealed associations of common genes with pathways related to *neurodegeneration-multiple diseases*, *fluid shear stress and atherosclerosis*, *lipid and atherosclerosis*, *Parkinson's disease*, and *prion diseases* (Fig. 5B–Table 4).

3.3. Construction of networks comprised of TFs and common genes

Utilizing the integrated data-mining tool ChIP-Atlas, we identified regulatory TFs with relevance to COVID-19 and PTB. Subsequently, we constructed an interaction network to elucidate regulatory signals between these predicted TFs and their common hub gene targets. Examination of the resulting interaction network (Fig. 6) revealed statistically significant interactions among predicted regulatory TFs and common hub gene targets.

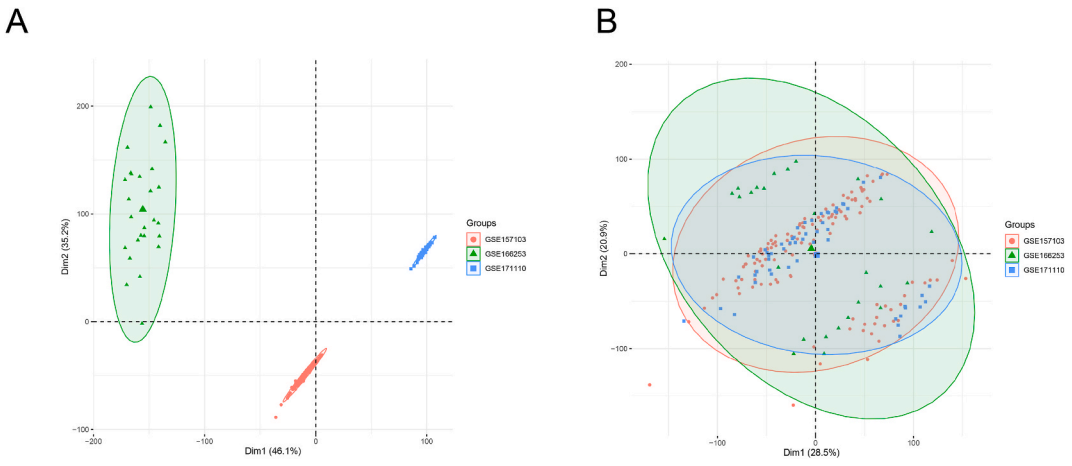

Fig. 2. PCA before and after batch effect elimination for all COVID-19 dataset samples. (A–B) Depiction of distributions of COVID-19 samples, with (A) representing the initial state and (B) illustrating the state after batch effect removal.

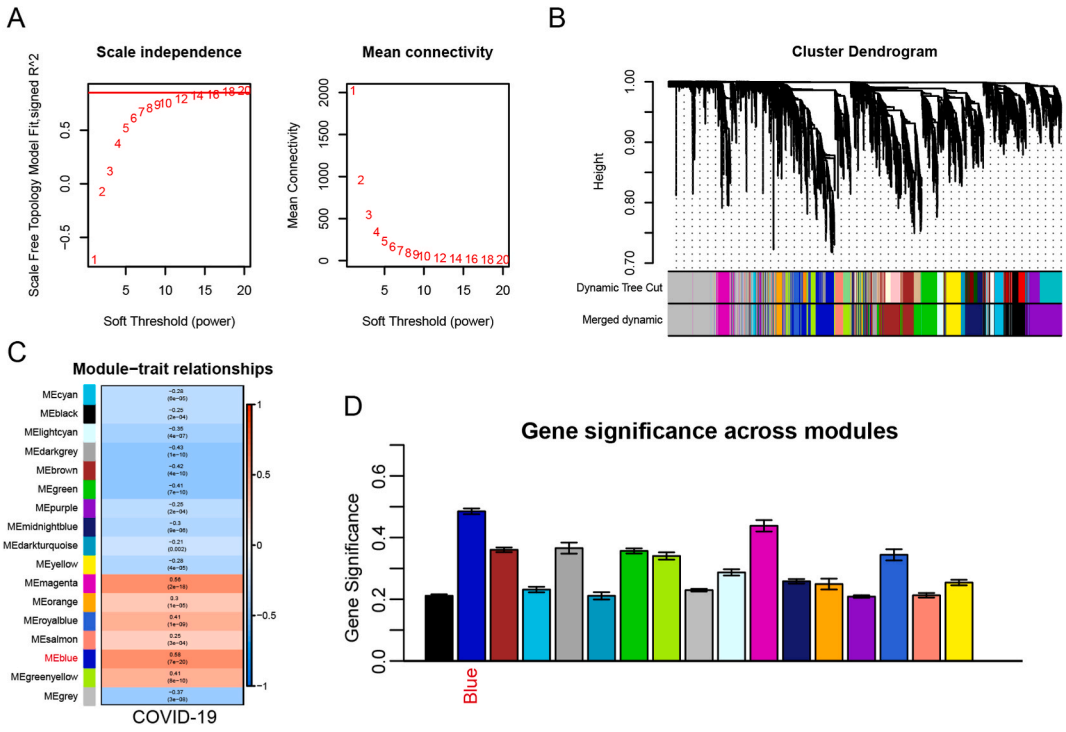

Fig. 3. Assessment of soft-thresholding power of WGCNA and identification of TB-related modules. (A) The scale-free fit index was examined across various soft-thresholding powers (left), and the mean connectivity was assessed for various powers (right). (B) Dendrogram showing clustering of all differentially expressed genes based on a dissimilarity measure (1-TOM). (C) Distribution of average gene significance and errors within the TB-associated modules. (D) Heatmap representing correlations between module eigengenes and TB.. (TOM: topological overlap matrix.)

Exploration of additional diseases strongly correlated with common genes associated with both COVID-19 and PTB.

Understanding relationships between genes and diseases is crucial for developing therapeutic treatments [13]. To uncover gene-disease relationships for COVID-19 and PTB, we relied on DisGeNET, a comprehensive platform that integrates and standardises data related to disease associations with genes and gene variants. Utilizing this resource, Table 1 show cases connections between genes and specific diseases. Our analysis unveiled common genes associated with both COVID-19 and PTB that exhibited the strongest correlations with three disorders: autosomal recessive chronic granulomatous disease, liver abscess, and peroxisome biogenesis disorder.

4. Results of real-time qPCR analysis

To confirm that common genes identified through our bioinformatics analysis are expressed in COVID-19 and PTB patients, we collected blood samples from patients and conducted real-time qPCR to quantify expression levels of these genes. The results showed that among the 11 common genes, the level of CALM3, CP2BP2, CYBA, DECR1, and FIG4 were significantly increased in both PTB and COVID-19 patients (Fig. 7). These findings strongly indicate that, these highly expressed genes identified in this study are pivotal hub genes associated with both PTB and COVID-19.

The accuracy and reliability of results from PCR-based molecular biological analyses, including real-time qPCR, depend on critical factors such as PCR amplification and dissociation curves. In this study, the shapes of these curves (Fig. S3) and the number of amplification cycles (Fig. S4) required for reliable results collectively indicated that high-quality cDNA was produced from patient blood samples and that our PCR primers possessed excellent specificity, further validating the authenticity and accuracy of our real-time qPCR results. Taken together, these findings suggest that the upregulation of the aforementioned common genes may contribute to the pathogenesis of patients afflicted with both COVID-19 and PTB.

4.1. Identification of candidate drugs for patients with both COVID-9 and PTB

Use of Enrichr and transcriptional signatures within the DSigDB database led to the identification of 473 drug molecules associated with common genes as potential treatments for PTB and COVID-19. The top 10 compounds were further screened using a P-value cutoff of 0.05 to identify potential novel therapeutic drug treatments for individuals afflicted with both COVID-19 and TB (Table 2).

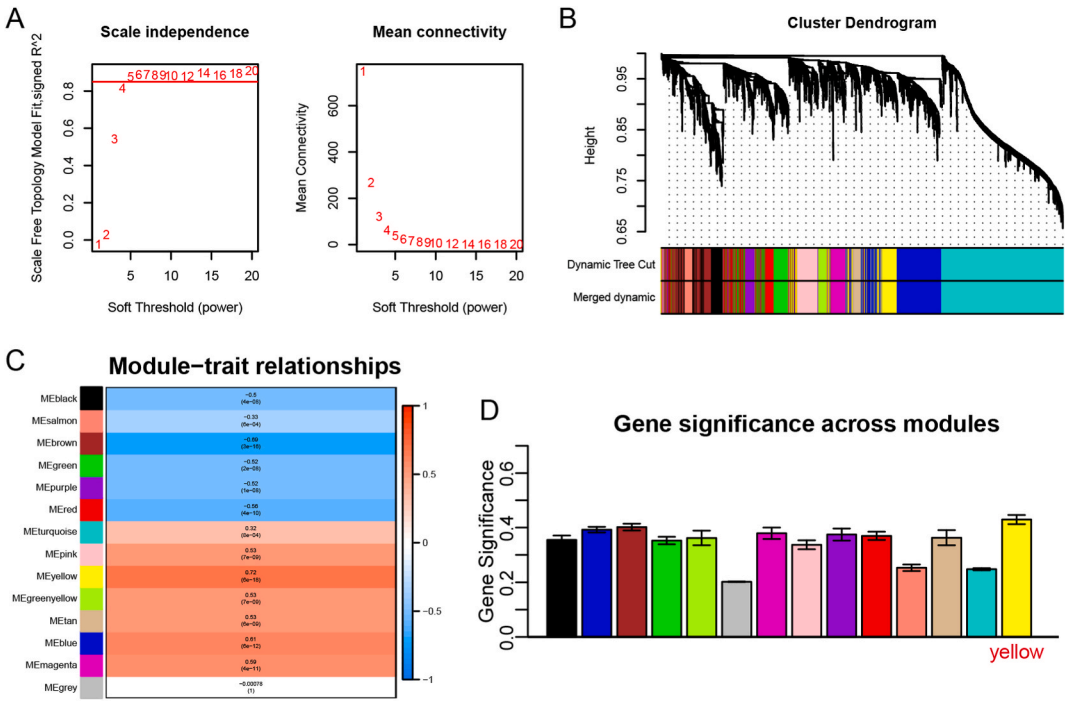

Fig. 4. Assessment of soft-thresholding power of WGCNA and identification of COVID-19-related modules. (A) The scale-free fit index was examined across various soft-thresholding powers (left) and the mean connectivity was assessed for various soft-thresholding powers (right). (B) Dendrogram showing clustering of all differentially expressed genes based on a dissimilarity measure (1-TOM). (C) Distribution of average gene significance and errors within COVID-19-associated modules (D) Heatmap representing correlations between module eigengenes and COVID-19. TOM: topological overlap matrix.

5. Discussion

As infectious diseases, both COVID-19 and TB trigger robust inflammatory responses that can potentially trigger cytokine storms and the development of various other disorders, including multiple organ failure. In their comprehensive meta-analysis, Sheerin et al. integrated transcriptomic data and insights from human macrophage infection studies to elucidate the immunopathogenic connections between COVID-19 and TB. Their analysis unveiled a bidirectional impact, with TB infection potentially exacerbating the severity of COVID-19 and vice versa, prompting the authors to suggest that established TB vaccines and treatments might serve as promising avenues to mitigate the severity of COVID-19. Furthermore, their findings underscore the dual risk associated with co-infections and emphasize the intricate interplay between these two infectious diseases [14].

It is crucial to note that the results of their meta-analysis should be validated using an alternative analytical approach. To address this need, we employed the WGCNA package, integrating data from separate COVID-19 and TB databases to pinpoint significant genes and modules associated with both diseases. Through this analysis, we identified 11 common genes associated with both COVID-19 and TB, providing valuable insights into the molecular mechanisms underlying SARS-CoV-2 and *Mtb* co-infection. To explore molecular mechanisms underlying susceptibility to co-infection, we conducted GO and KEGG pathway enrichment analyses.

Our results revealed that the GO biological process (BP) term *RNA splicing* was strongly associated with functions of these 11 common genes, indicating that this process is strongly linked to pathogenic mechanisms of both COVID-19 and PTB. Notably, viruses like SARS-CoV-2 manipulate host splicing to bolster replication [15–17], while in PTB, splicing plays regulatory roles in both the host immune response and pathogen survival [18,19]. Therefore, targeting of splicing factors may impede viral or bacterial replication and enhance immune responses.

With regard to cellular components (CC), common genes were linked to GO functional terms *granule membrane* and *vesicle membrane*, suggesting involvement of extracellular vesicles (EVs) in both diseases. EVs have been reported to transport viral and bacterial components, modulate immune responses, and participate in disease progression [20,21]. Nevertheless, further research is needed to fully understand the intricate relationship between EVs and pathogenesis of COVID-19 and PTB.

In terms of molecular function (MF), several common genes exhibited notably strong associations with the KEGG pathway term *phosphatidylinositol 3-kinase*, indicating these genes are significantly associated with pathways related to neurodegeneration and various other disorders. Intriguingly, both COVID-19 and TB have been associated with neurodegeneration, with COVID-19 linked to neurological symptoms and long-term cognitive impairments [22] and TB linked to central nervous system-related neurological complications [23]. Mechanistically, these diseases may promote neurodegeneration by triggering inflammation, oxidative stress, and immune dysregulation [22,24]. However, further research is needed to unravel the intricate interplay between COVID-19, TB and

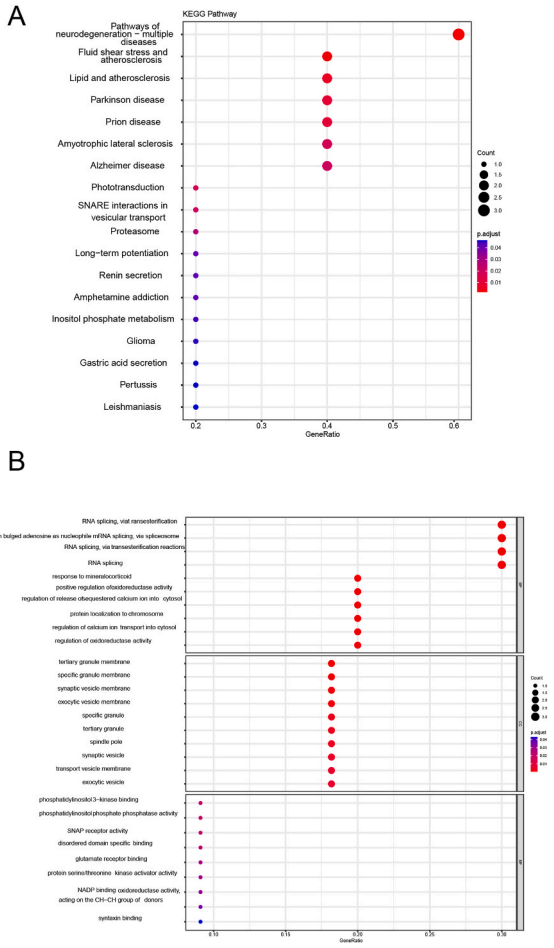

Fig. 5. Results of functional analysis of genes shared by COVID-19 and PTB. (A) Gene Ontology (GO) enrichment analysis. (B) Kyoto Encyclopedia of Genes and Genomes (KEGG) enrichment analysis. BP: biological process; CC: cellular component; MF: molecular function.

Table 1
Prediction of top 10 diseases associated with COVID -19 and TB coinfection.

Disease name	P-value	Genes
Autosomal Recessive Chronic Granulomatous Disease	7.69E-06	CYBA; DECR1
Liver Abscess	7.69E-06	CYBA; DECR1
Peroxisome Biogenesis Disorder, Complementation Group D	2.88E-05	CYBA; DECR1
Disease of capillaries	1.11E-04	CYBA; DECR1
Pre-renal acute kidney injury	1.62E-04	CYBA; DECR1
Granulomatous Disease, Chronic, X-Linked	2.69E-04	CYBA; DECR1
Acute periodontitis	2.81E-04	CYBA; DECR1
Pyloric Stenosis	2.81E-04	FIG4; CYBA
Diabetic Cardiomyopathies	3.87E-04	CALM3; DECR1
Essential Hypertension	4.04E-04	CYBA; CALM3; DECR1

neurodegeneration.

TFs are proteins that exert their regulatory influence on gene expression by first binding to specific DNA sequences. In this study, we employed the Cytoscape package to pinpoint TFs that regulate expression of 11 common genes associated with both COVID-19 and PTB pathogenic mechanisms. Ultimately, our results confirmed that 10 of these genes were potentially associated with these diseases.

CALM3, a potential protease, may facilitate viral invasion [25]. *CYBA* encodes a crucial subunit needed for NADPH oxidase (NOX) complex activation and localization and thus potentially plays a pivotal role in regulating oxidase activity. NOX is a multiprotein complex that produces reactive oxygen species (ROS) in phagocytic cells, such as neutrophils and macrophages. Given that NOX-generated ROS are pivotal players in the immune response, SARS-CoV-2 and *Mtb* infections may trigger acute host oxidative stress responses that eliminate these pathogens. However, excess ROS production can lead to an uncontrolled inflammatory response

Table 2
Prediction of top 10 candidate drugs for COVID -19 and TB coinfection.

Name of drugs	P-value	Adjusted P-value	Genes
VITAMIN E CTD 00006994	6.08E-05	0.028765136	FIG4; IK; CD2BP2; CYBA; CALM3; IFFO1
meglumine PC3 DOWN	1.27E-04	0.029980743	IK; VAMP1
trichostatin A HL60 UP	3.35E-04	0.052891665	FIG4; IK; VAMP1; CALM3
vorinostat HL60 UP	4.66E-04	0.055075264	FIG4; IK; VAMP1; CALM3
SELENIUM CTD 00006731	8.86E-04	0.077267101	FIG4; PSMD6; IK; CD2BP2; CALM3
NADP(+) BOSS	9.80E-04	0.077267101	CYBA; DECR1
2-Methylcholine CTD 00002006	0.001201048	0.081156524	IK; VAMP1; CD2BP2; IFFO1; DECR1
tolazoline PC3 DOWN	0.003056146	0.115340128	IK; VAMP1
sulfaguanidine PC3 DOWN	0.003413508	0.115340128	IK; VAMP1; CD2BP2
ALDOSTERONE BOSS	0.004019697	0.115340128	CYBA; DECR1
Superoxide BOSS	0.004619219	0.115340128	CYBA; DECR1
streptozocin BOSS	0.004714931	0.115340128	CYBA; DECR1
1-Phosphatidyl-myo-inositol BOSS	0.004763133	0.115340128	FIG4; DECR1
Angiotensin II, human BOSS	0.004811565	0.115340128	CYBA; DECR1
ramipril CTD 00007148	0.006034819	0.115340128	CYBA
parthenolide MCF7 UP	0.006370552	0.115340128	CD2BP2; RBM23
Hexylene glycol TTD 00008431	0.006581796	0.115340128	CALM3
Tetradecanoic acid TTD 00011406	0.006581796	0.115340128	CALM3
2-Aminobiphenyl CTD 00000776	0.006581796	0.115340128	CYBA

that can damage the host. As such, common genes *CYBA* and *CD2BP2* may play key roles in COVID-19-induced cytokine storm, with *CD2BP2* initially reported to bind to two conserved proline-rich motifs in the cytoplasmic tail of the T cell adhesion molecule CD2 [26].

FIG4 has been reported to interact with various steroid nuclear receptors, resulting in increased transcription of steroid-responsive genes in a hormone-dependent manner, although their specific functions remain unclear. *DECR1*, as a rate-limiting enzyme in an auxiliary pathway for polyunsaturated fatty acidβ-oxidation, widely expressed in a variety of malignancies. Various studies had reported that the high expression of DECR1 is closely related to the development of malignancy [27]. However, the role of both COVID-19 and TB is unclear.

After assigning putative functions to the 11 common genes, we conducted a thorough search in the DSigDB database to identify drugs with potential interactions with these genes in order to pinpoint candidate drug treatments for both COVID-19 and TB. The drug candidates with the top 10 significance scores are discussed below.

One noteworthy drug candidate, vitamin E, plays an important role in innate and adaptive immune systems by orchestrating immune responses and regulating the production of various immune cell types [28]. Notably, vitamin E supplementation has been shown to reduce lung-related pathology and mortality in mice with influenza by activating the Th1 cytokine response, resulting in enhanced pro-inflammatory responses for combatting the influenza virus [29].

Other drug candidates include histone deacetylase (HDAC) inhibitors, which have been reported to induce cancer cell cycle arrest, differentiation and cell death, reduce angiogenesis, and modulate the immune response. Examples of clinically useful HDACs include trichostatin A (TSA) and vorinostat, which are commonly administered as anti-tumour therapies. Intriguingly, recent studies have demonstrated that TSA may ameliorate Alzheimer's disease-associated pathology and cognitive deficits [30]. Based on our KEGG analysis results, it appears that individuals afflicted with both COVID-19 and PTB have heightened susceptibility to neurodegenerative diseases.

Another promising drug candidate is selenium, an essential trace element that regulates immune functions through its redox-regulating effects on selenoproteins, which protect immune cells from oxidative stress [31]. Selenium plays a crucial role in initiating and modulating immune responses, thereby alleviating excessive immune reactions and mitigating chronic inflammation [32]. Moreover, selenium is commonly employed as an anti-tumour therapy [33]. The safety and efficacy of these drugs for co-infected patients require validation through a comprehensive series of experiments. As SARS-CoV-2 is a new virus, less research has been done so far. This is the reason for collecting less number of samples for analyzing the results. In future, if more samples are available, the current study would be more effective in the context of the SARS-CoV-2 pandemic.

To understand the relationship between genes and diseases, we constructed a gene-disease interaction network for common genes related to COVID-19 and PTB to guide the selection of potential drug treatments for patients afflicted with both of these diseases. The results of this analysis revealed connections between these genes and other disorders, including liver abscess, peroxisome biogenesis disorder, capillary diseases, and other granulomatous diseases.

With regard to liver abscess, COVID-19 and TB patients commonly experience gastrointestinal symptoms, night sweats, cough, and weight loss, all of which are associated with both liver abscess and TB. Notably, liver abscess has been reported in a COVID-19 patient [34].

With regard to peroxisome biogenesis disorder, Roczkowsky et al. reported sustained COVID-19-induced neuroinflammatory responses accompanied by peroxisome biogenesis factor suppression, despite limited brainstem SARS-CoV-2 neurotropism in humans [35]. Additionally, *Mtb* acetyltransferase has been reported to suppress oxidative stress by inducing peroxisome formation in macrophages [36]. Therefore, individuals suffering from both COVID-19 and TB may have elevated risk of developing peroxisome biogenesis disorder.

In summary, we utilized WGCNA as a powerful tool to explore the relationship between COVID-19 and PTB. WGCNA is a well-

Table 3
GO terms of common gene for COVID-19 and PTB.

	ONTOLOGY	ID	Description	GeneRatio	BgRatio	pvalue	p.adjust	qvalue	geneID	Count
GO:0051385	BP	GO:0051385	response to mineralocorticoid	February 10, 2023	36/18723	0.000160195	0.000160195	0.026547919	CYBA/CALM3	2
GO:0051353	BP	GO:0051353	positive regulation of oxidoreductase activity	February 10, 2023	59/18723	0.000432226	0.000432226	0.026547919	CYBA/CALM3	2
GO:0000377	BP	GO:0000377	RNA splicing, via transesterification reactions with bulged adenosine as nucleophile	March 10, 2023	320/18723	0.000542914	0.000542914	0.026547919	RBM23/IK/CD2BP2	3
GO:0000398	BP	GO:0000398	mRNA splicing, via spliceosome	March 10, 2023	320/18723	0.000542914	0.000542914	0.026547919	RBM23/IK/CD2BP2	3
GO:0000375	BP	GO:0000375	RNA splicing, via transesterification reactions	March 10, 2023	324/18723	0.000562958	0.000562958	0.026547919	RBM23/IK/CD2BP2	3
GO:0051279	BP	GO:0051279	regulation of release of sequestered calcium ion into cytosol	February 10, 2023	79/18723	0.000773886	0.000773886	0.030412353	CYBA/CALM3	2
GO:0034502	BP	GO:0034502	protein localization to chromosome	February 10, 2023	92/18723	0.001047551	0.001047551	0.030844213	IK/IFFO1	2
GO:0010522	BP	GO:0010522	regulation of calcium ion transport into cytosol	February 10, 2023	102/18723	0.001285374	0.001285374	0.030844213	CYBA/CALM3	2
GO:0008380	BP	GO:0008380	RNA splicing	March 10, 2023	434/18723	0.001314664	0.001314664	0.030844213	RBM23/IK/CD2BP2	3
GO:0051341	BP	GO:0051341	regulation of oxidoreductase activity	February 10, 2023	107/18723	0.001413119	0.001413119	0.030844213	CYBA/CALM3	2
GO:0051209	BP	GO:0051209	release of sequestered calcium ion into cytosol	February 10, 2023	115/18723	0.001629677	0.001629677	0.030844213	CYBA/CALM3	2
GO:0051283	BP	GO:0051283	negative regulation of sequestering of calcium ion	February 10, 2023	116/18723	0.001657795	0.001657795	0.030844213	CYBA/CALM3	2
GO:0051282	BP	GO:0051282	regulation of sequestering of calcium ion	February 10, 2023	118/18723	0.001714728	0.001714728	0.030844213	CYBA/CALM3	2
GO:0051208	BP	GO:0051208	sequestering of calcium ion	February 10, 2023	122/18723	0.001831375	0.001831375	0.030844213	CYBA/CALM3	2
GO:0097553	BP	GO:0097553	calcium ion transmembrane import into cytosol	February 10, 2023	142/18723	0.002469809	0.002469809	0.038823669	CYBA/CALM3	2
GO:1903169	BP	GO:1903169	regulation of calcium ion transmembrane transport	February 10, 2023	159/18723	0.003083936	0.003083936	0.043303189	CYBA/CALM3	2
GO:0060402	BP	GO:0060402	calcium ion transport into cytosol	February 10, 2023	160/18723	0.003122083	0.003122083	0.043303189	CYBA/CALM3	2
GO:0031960	BP	GO:0031960	response to corticosteroid	February 10, 2023	167/18723	0.003395354	0.003395354	0.044477155	CYBA/CALM3	2
GO:0060401	BP	GO:0060401	cytosolic calcium ion transport	February 10, 2023	182/18723	0.004017474	0.004017474	0.049856745	CYBA/CALM3	2
GO:1901654	BP	GO:1901654	response to ketone	February 10, 2023	194/18723	0.004550679	0.004550679	0.05365011	CYBA/CALM3	2
GO:0030258	BP	GO:0030258	lipid modification	February 10, 2023	212/18723	0.005408868	0.005408868	0.059038526	FIG4/DECR1	2
GO:0051651	BP	GO:0051651	maintenance of location in cell	February 10, 2023	214/18723	0.005508505	0.005508505	0.059038526	CYBA/CALM3	2
GO:0097305	BP	GO:0097305	response to alcohol	February 10, 2023	253/18723	0.007619585	0.007619585	0.069689928	CYBA/CALM3	2
GO:0051924	BP	GO:0051924	regulation of calcium ion transport	February 10, 2023	255/18723	0.007736355	0.007736355	0.069689928	CYBA/CALM3	2

(*continued on next page*)

Table 3 (*continued*)

	ONTOLOGY	ID	Description	GeneRatio	BgRatio	pvalue	p.adjust	qvalue	geneID	Count
GO:0070588	BP	GO:0070588	calcium ion transmembrane transport	February 10, 2023	312/18723	0.011402944	0.011402944	0.069689928	CYBA/CALM3	2
GO:0007204	BP	GO:0007204	positive regulation of cytosolic calcium ion concentration	February 10, 2023	319/18723	0.011897416	0.011897416	0.069689928	CYBA/CALM3	2
GO:0051235	BP	GO:0051235	maintenance of location	February 10, 2023	327/18723	0.012474098	0.012474098	0.069689928	CYBA/CALM3	2
GO:0048545	BP	GO:0048545	response to steroid hormone	February 10, 2023	339/18723	0.013362064	0.013362064	0.069689928	CYBA/CALM3	2
GO:0051480	BP	GO:0051480	regulation of cytosolic calcium ion concentration	February 10, 2023	353/18723	0.014432451	0.014432451	0.069689928	CYBA/CALM3	2
GO:1904062	BP	GO:1904062	regulation of cation transmembrane transport	February 10, 2023	357/18723	0.01474502	0.01474502	0.069689928	CYBA/CALM3	2
GO:0010800	BP	GO:0010800	positive regulation of peptidyl-threonine phosphorylation	January 10, 2023	30/18723	0.01591183	0.01591183	0.069689928	CALM3	1
GO:0010880	BP	GO:0010880	regulation of release of sequestered calcium ion into cytosol by sarcoplasmic reticulum	January 10, 2023	30/18723	0.01591183	0.01591183	0.069689928	CALM3	1
GO:0090151	BP	GO:0090151	establishment of protein localization to mitochondrial membrane	January 10, 2023	30/18723	0.01591183	0.01591183	0.069689928	CALM3	1
GO:0007190	BP	GO:0007190	activation of adenylate cyclase activity	January 10, 2023	31/18723	0.016438278	0.016438278	0.069689928	CALM3	1
GO:0071480	BP	GO:0071480	cellular response to gamma radiation	January 10, 2023	31/18723	0.016438278	0.016438278	0.069689928	CYBA	1
GO:0010644	BP	GO:0010644	cell communication by electrical coupling	January 10, 2023	32/18723	0.016964472	0.016964472	0.069689928	CALM3	1
GO:0046856	BP	GO:0046856	phosphatidylinositol dephosphorylation	January 10, 2023	32/18723	0.016964472	0.016964472	0.069689928	FIG4	1
GO:0001975	BP	GO:0001975	response to amphetamine	January 10, 2023	33/18723	0.017490412	0.017490412	0.069689928	CALM3	1
GO:0010922	BP	GO:0010922	positive regulation of phosphatase activity	January 10, 2023	34/18723	0.018016099	0.018016099	0.069689928	CALM3	1
GO:0014808	BP	GO:0014808	release of sequestered calcium ion into cytosol by sarcoplasmic reticulum	January 10, 2023	34/18723	0.018016099	0.018016099	0.069689928	CALM3	1
GO:0032770	BP	GO:0032770	positive regulation of monooxygenase activity	January 10, 2023	34/18723	0.018016099	0.018016099	0.069689928	CALM3	1
GO:0098801	BP	GO:0098801	regulation of renal system process	January 10, 2023	35/18723	0.018541534	0.018541534	0.069689928	CYBA	1
GO:1903514	BP	GO:1903514	release of sequestered calcium ion into cytosol by endoplasmic reticulum	January 10, 2023	35/18723	0.018541534	0.018541534	0.069689928	CALM3	1
GO:0010959	BP	GO:0010959	regulation of metal ion transport	February 10, 2023	406/18723	0.018812092	0.018812092	0.069689928	CYBA/CALM3	2
GO:0017004	BP	GO:0017004	cytochrome complex assembly	January 10, 2023	36/18723	0.019066715	0.019066715	0.069689928	CYBA	1
GO:0090322	BP	GO:0090322	regulation of superoxide metabolic process	January 10, 2023	36/18723	0.019066715	0.019066715	0.069689928	CYBA	1
GO:0001990	BP	GO:0001990	regulation of systemic arterial blood pressure by hormone	January 10, 2023	37/18723	0.019591643	0.019591643	0.069689928	CYBA	1
GO:0045730	BP	GO:0045730	respiratory burst	January 10, 2023	37/18723	0.019591643	0.019591643	0.069689928	CYBA	1
GO:0016311	BP	GO:0016311	dephosphorylation	February 10, 2023	417/18723	0.01978438	0.01978438	0.069689928	FIG4/CALM3	2

(*continued on next page*)

Table 3 (*continued*)

	ONTOLOGY	ID	Description	GeneRatio	BgRatio	pvalue	p.adjust	qvalue	geneID	Count
GO:0007094	BP	GO:0007094	mitotic spindle assembly checkpoint signaling	January 10, 2023	38/ 18723	0.020116318	0.020116318	0.069689928	IK	1
GO:0032941	BP	GO:0032941	secretion by tissue	January 10, 2023	38/ 18723	0.020116318	0.020116318	0.069689928	CYBA	1
GO:0071173	BP	GO:0071173	spindle assembly checkpoint signaling	January 10, 2023	38/ 18723	0.020116318	0.020116318	0.069689928	IK	1
GO:0071174	BP	GO:0071174	mitotic spindle checkpoint signaling	January 10, 2023	38/ 18723	0.020116318	0.020116318	0.069689928	IK	1
GO:0006816	BP	GO:0006816	calcium ion transport	February 10, 2023	422/ 18723	0.020233362	0.020233362	0.069689928	CYBA/CALM3	2
GO:0044772	BP	GO:0044772	mitotic cell cycle phase transition	February 10, 2023	424/ 18723	0.020414178	0.020414178	0.069689928	IK/CALM3	2
GO:0031577	BP	GO:0031577	spindle checkpoint signaling	January 10, 2023	39/ 18723	0.020640741	0.020640741	0.069689928	IK	1
GO:1901021	BP	GO:1901021	positive regulation of calcium ion transmembrane transporter activity	January 10, 2023	39/ 18723	0.020640741	0.020640741	0.069689928	CALM3	1
GO:0045777	BP	GO:0045777	positive regulation of blood pressure	January 10, 2023	40/ 18723	0.021164911	0.021164911	0.069689928	CYBA	1
GO:0045841	BP	GO:0045841	negative regulation of mitotic metaphase/anaphase transition	January 10, 2023	40/ 18723	0.021164911	0.021164911	0.069689928	IK	1
GO:0051281	BP	GO:0051281	positive regulation of release of sequestered calcium ion into cytosol	January 10, 2023	40/ 18723	0.021164911	0.021164911	0.069689928	CALM3	1
GO:1901020	BP	GO:1901020	negative regulation of calcium ion transmembrane transporter activity	January 10, 2023	40/ 18723	0.021164911	0.021164911	0.069689928	CALM3	1
GO:0070296	BP	GO:0070296	sarcoplasmic reticulum calcium ion transport	January 10, 2023	41/ 18723	0.021688828	0.021688828	0.069689928	CALM3	1
GO:1901385	BP	GO:1901385	regulation of voltage-gated calcium channel activity	January 10, 2023	41/ 18723	0.021688828	0.021688828	0.069689928	CALM3	1
GO:1902100	BP	GO:1902100	negative regulation of metaphase/anaphase transition of cell cycle	January 10, 2023	42/ 18723	0.022212494	0.022212494	0.069689928	IK	1
GO:0006874	BP	GO:0006874	cellular calcium ion homeostasis	February 10, 2023	448/ 18723	0.022637959	0.022637959	0.069689928	CYBA/CALM3	2
GO:0031952	BP	GO:0031952	regulation of protein autophosphorylation	January 10, 2023	43/ 18723	0.022735906	0.022735906	0.069689928	CALM3	1
GO:0033046	BP	GO:0033046	negative regulation of sister chromatid segregation	January 10, 2023	43/ 18723	0.022735906	0.022735906	0.069689928	IK	1
GO:0033048	BP	GO:0033048	negative regulation of mitotic sister chromatid segregation	January 10, 2023	43/ 18723	0.022735906	0.022735906	0.069689928	IK	1
GO:2000816	BP	GO:2000816	negative regulation of mitotic sister chromatid separation	January 10, 2023	43/ 18723	0.022735906	0.022735906	0.069689928	IK	1
GO:0003012	BP	GO:0003012	muscle system process	February 10, 2023	452/ 18723	0.023018183	0.023018183	0.069689928	CYBA/CALM3	2
GO:0021762	BP	GO:0021762	substantia nigra development	January 10, 2023	44/ 18723	0.023259067	0.023259067	0.069689928	CALM3	1
GO:0042554	BP	GO:0042554	superoxide anion generation	January 10, 2023	44/ 18723	0.023259067	0.023259067	0.069689928	CYBA	1
GO:0050999	BP	GO:0050999	regulation of nitric-oxide synthase activity	January 10, 2023	44/ 18723	0.023259067	0.023259067	0.069689928	CALM3	1
GO:0062208	BP	GO:0062208	positive regulation of pattern recognition receptor signaling pathway	January 10, 2023	44/ 18723	0.023259067	0.023259067	0.069689928	CYBA	1

(*continued on next page*)

Table 3 (*continued*)

	ONTOLOGY	ID	Description	GeneRatio	BgRatio	pvalue	p.adjust	qvalue	geneID	Count
GO:0035307	BP	GO:0035307	positive regulation of protein dephosphorylation	January 10, 2023	45/ 18723	0.023781976	0.023781976	0.069689928	CALM3	1
GO:0051985	BP	GO:0051985	negative regulation of chromosome segregation	January 10, 2023	45/ 18723	0.023781976	0.023781976	0.069689928	IK	1
GO:1905819	BP	GO:1905819	negative regulation of chromosome separation	January 10, 2023	45/ 18723	0.023781976	0.023781976	0.069689928	IK	1
GO:0055074	BP	GO:0055074	calcium ion homeostasis	February 10, 2023	460/ 18723	0.023786757	0.023786757	0.069689928	CYBA/CALM3	2
GO:0033047	BP	GO:0033047	regulation of mitotic sister chromatid segregation	January 10, 2023	46/ 18723	0.024304632	0.024304632	0.069689928	IK	1
GO:0046839	BP	GO:0046839	phospholipid dephosphorylation	January 10, 2023	46/ 18723	0.024304632	0.024304632	0.069689928	FIG4	1
GO:0003044	BP	GO:0003044	regulation of systemic arterial blood pressure mediated by a chemical signal	January 10, 2023	47/ 18723	0.024827037	0.024827037	0.069689928	CYBA	1
GO:0010799	BP	GO:0010799	regulation of peptidyl-threonine phosphorylation	January 10, 2023	47/ 18723	0.024827037	0.024827037	0.069689928	CALM3	1
GO:0031641	BP	GO:0031641	regulation of myelination	January 10, 2023	47/ 18723	0.024827037	0.024827037	0.069689928	FIG4	1
GO:1903170	BP	GO:1903170	negative regulation of calcium ion transmembrane transport	January 10, 2023	47/ 18723	0.024827037	0.024827037	0.069689928	CALM3	1
GO:0045839	BP	GO:0045839	negative regulation of mitotic nuclear division	January 10, 2023	48/ 18723	0.02534919	0.02534919	0.070318496	IK	1
GO:0014075	BP	GO:0014075	response to amine	January 10, 2023	49/ 18723	0.025871091	0.025871091	0.070456363	CALM3	1
GO:0072503	BP	GO:0072503	cellular divalent inorganic cation homeostasis	February 10, 2023	486/ 18723	0.026358502	0.026358502	0.070456363	CYBA/CALM3	2
GO:0000387	BP	GO:0000387	spliceosomal snRNP assembly	January 10, 2023	50/ 18723	0.026392741	0.026392741	0.070456363	CD2BP2	1
GO:0034765	BP	GO:0034765	regulation of ion transmembrane transport	February 10, 2023	491/ 18723	0.026865855	0.026865855	0.070456363	CYBA/CALM3	2
GO:1903426	BP	GO:1903426	regulation of reactive oxygen species biosynthetic process	January 10, 2023	52/ 18723	0.027435287	0.027435287	0.070456363	CYBA	1
GO:0031279	BP	GO:0031279	regulation of cyclase activity	January 10, 2023	53/ 18723	0.027956183	0.027956183	0.070456363	CALM3	1
GO:0010524	BP	GO:0010524	positive regulation of calcium ion transport into cytosol	January 10, 2023	54/ 18723	0.028476827	0.028476827	0.070456363	CALM3	1
GO:0070839	BP	GO:0070839	metal ion export	January 10, 2023	54/ 18723	0.028476827	0.028476827	0.070456363	CALM3	1
GO:2000300	BP	GO:2000300	regulation of synaptic vesicle exocytosis	January 10, 2023	54/ 18723	0.028476827	0.028476827	0.070456363	CALM3	1
GO:0098900	BP	GO:0098900	regulation of action potential	January 10, 2023	55/ 18723	0.028997221	0.028997221	0.070456363	CALM3	1
GO:0010332	BP	GO:0010332	response to gamma radiation	January 10, 2023	56/ 18723	0.029517364	0.029517364	0.070456363	CYBA	1
GO:0043388	BP	GO:0043388	positive regulation of DNA binding	January 10, 2023	56/ 18723	0.029517364	0.029517364	0.070456363	CALM3	1
GO:0051784	BP	GO:0051784	negative regulation of nuclear division	January 10, 2023	56/ 18723	0.029517364	0.029517364	0.070456363	IK	1
GO:0042743	BP	GO:0042743	hydrogen peroxide metabolic process	January 10, 2023	58/ 18723	0.030556898	0.030556898	0.070456363	CYBA	1

(*continued on next page*)

Table 3 (*continued*)

	ONTOLOGY	ID	Description	GeneRatio	BgRatio	pvalue	p.adjust	qvalue	geneID	Count
GO:0043666	BP	GO:0043666	regulation of phosphoprotein phosphatase activity	January 10, 2023	58/18723	0.030556898	0.030556898	0.070456363	CALM3	1
GO:0086065	BP	GO:0086065	cell communication involved in cardiac conduction	January 10, 2023	58/18723	0.030556898	0.030556898	0.070456363	CALM3	1
GO:0032768	BP	GO:0032768	regulation of monooxygenase activity	January 10, 2023	59/18723	0.031076289	0.031076289	0.070456363	CALM3	1
GO:0035306	BP	GO:0035306	positive regulation of dephosphorylation	January 10, 2023	59/18723	0.031076289	0.031076289	0.070456363	CALM3	1
GO:2001258	BP	GO:2001258	negative regulation of cation channel activity	January 10, 2023	59/18723	0.031076289	0.031076289	0.070456363	CALM3	1
GO:0030071	BP	GO:0030071	regulation of mitotic metaphase/anaphase transition	January 10, 2023	60/18723	0.031595429	0.031595429	0.070543775	IK	1
GO:0007091	BP	GO:0007091	metaphase/anaphase transition of mitotic cell cycle	January 10, 2023	62/18723	0.032632959	0.032632959	0.070543775	IK	1
GO:0048488	BP	GO:0048488	synaptic vesicle endocytosis	January 10, 2023	62/18723	0.032632959	0.032632959	0.070543775	CALM3	1
GO:0140238	BP	GO:0140238	presynaptic endocytosis	January 10, 2023	62/18723	0.032632959	0.032632959	0.070543775	CALM3	1
GO:1902099	BP	GO:1902099	regulation of metaphase/anaphase transition of cell cycle	January 10, 2023	63/18723	0.033151349	0.033151349	0.070543775	IK	1
GO:0046854	BP	GO:0046854	phosphatidylinositol phosphate biosynthetic process	January 10, 2023	64/18723	0.033669488	0.033669488	0.070543775	FIG4	1
GO:0048857	BP	GO:0048857	neural nucleus development	January 10, 2023	64/18723	0.033669488	0.033669488	0.070543775	CALM3	1
GO:1903409	BP	GO:1903409	reactive oxygen species biosynthetic process	January 10, 2023	64/18723	0.033669488	0.033669488	0.070543775	CYBA	1
GO:0010965	BP	GO:0010965	regulation of mitotic sister chromatid separation	January 10, 2023	65/18723	0.034187378	0.034187378	0.070543775	IK	1
GO:0044784	BP	GO:0044784	metaphase/anaphase transition of cell cycle	January 10, 2023	65/18723	0.034187378	0.034187378	0.070543775	IK	1
GO:0006303	BP	GO:0006303	double-strand break repair via nonhomologous end joining	January 10, 2023	66/18723	0.034705018	0.034705018	0.070543775	IFFO1	1
GO:0050766	BP	GO:0050766	positive regulation of phagocytosis	January 10, 2023	66/18723	0.034705018	0.034705018	0.070543775	CYBA	1
GO:0051306	BP	GO:0051306	mitotic sister chromatid separation	January 10, 2023	67/18723	0.035222408	0.035222408	0.070679581	IK	1
GO:0051926	BP	GO:0051926	negative regulation of calcium ion transport	January 10, 2023	68/18723	0.035739549	0.035739549	0.070679581	CALM3	1
GO:0071230	BP	GO:0071230	cellular response to amino acid stimulus	January 10, 2023	71/18723	0.037289474	0.037289474	0.070679581	CYBA	1
GO:0033045	BP	GO:0033045	regulation of sister chromatid segregation	January 10, 2023	72/18723	0.037805618	0.037805618	0.070679581	IK	1
GO:0071479	BP	GO:0071479	cellular response to ionizing radiation	January 10, 2023	72/18723	0.037805618	0.037805618	0.070679581	CYBA	1
GO:1905818	BP	GO:1905818	regulation of chromosome separation	January 10, 2023	72/18723	0.037805618	0.037805618	0.070679581	IK	1
GO:0050848	BP	GO:0050848	regulation of calcium-mediated signaling	January 10, 2023	73/18723	0.038321512	0.038321512	0.070679581	CALM3	1
GO:1904427	BP	GO:1904427	positive regulation of calcium ion transmembrane transport	January 10, 2023	73/18723	0.038321512	0.038321512	0.070679581	CALM3	1

(*continued on next page*)

Table 3 (*continued*)

	ONTOLOGY	ID	Description	GeneRatio	BgRatio	pvalue	p.adjust	qvalue	geneID	Count
GO:0006635	BP	GO:0006635	fatty acid beta-oxidation	January 10, 2023	74/18723	0.038837157	0.038837157	0.070679581	DECR1	1
GO:0006801	BP	GO:0006801	superoxide metabolic process	January 10, 2023	74/18723	0.038837157	0.038837157	0.070679581	CYBA	1
GO:0034121	BP	GO:0034121	regulation of toll-like receptor signaling pathway	January 10, 2023	75/18723	0.039352554	0.039352554	0.070679581	CYBA	1
GO:0036465	BP	GO:0036465	synaptic vesicle recycling	January 10, 2023	75/18723	0.039352554	0.039352554	0.070679581	CALM3	1
GO:2001259	BP	GO:2001259	positive regulation of cation channel activity	January 10, 2023	75/18723	0.039352554	0.039352554	0.070679581	CALM3	1
GO:0014823	BP	GO:0014823	response to activity	January 10, 2023	76/18723	0.039867701	0.039867701	0.070679581	CYBA	1
GO:0086001	BP	GO:0086001	cardiac muscle cell action potential	January 10, 2023	76/18723	0.039867701	0.039867701	0.070679581	CALM3	1
GO:0140115	BP	GO:0140115	export across plasma membrane	January 10, 2023	76/18723	0.039867701	0.039867701	0.070679581	CALM3	1
GO:2000379	BP	GO:2000379	positive regulation of reactive oxygen species metabolic process	January 10, 2023	76/18723	0.039867701	0.039867701	0.070679581	CYBA	1
GO:0055117	BP	GO:0055117	regulation of cardiac muscle contraction	January 10, 2023	77/18723	0.0403826	0.0403826	0.07105815	CALM3	1
GO:0071229	BP	GO:0071229	cellular response to acid chemical	January 10, 2023	80/18723	0.041925807	0.041925807	0.07322714	CYBA	1
GO:0071260	BP	GO:0071260	cellular response to mechanical stimulus	January 10, 2023	81/18723	0.042439712	0.042439712	0.073579687	CYBA	1
GO:0050000	BP	GO:0050000	chromosome localization	January 10, 2023	82/18723	0.04295337	0.04295337	0.073926661	IFFO1	1
GO:0050886	BP	GO:0050886	endocrine process	January 10, 2023	83/18723	0.043466779	0.043466779	0.074268182	CYBA	1
GO:0010921	BP	GO:0010921	regulation of phosphatase activity	January 10, 2023	84/18723	0.043979941	0.043979941	0.074604368	CALM3	1
GO:0032413	BP	GO:0032413	negative regulation of ion transmembrane transporter activity	January 10, 2023	86/18723	0.045005521	0.045005521	0.074731184	CALM3	1
GO:0046928	BP	GO:0046928	regulation of neurotransmitter secretion	January 10, 2023	86/18723	0.045005521	0.045005521	0.074731184	CALM3	1
GO:2001251	BP	GO:2001251	negative regulation of chromosome organization	January 10, 2023	86/18723	0.045005521	0.045005521	0.074731184	IK	1
GO:0030901	BP	GO:0030901	midbrain development	January 10, 2023	90/18723	0.047053711	0.047053711	0.076245898	CALM3	1
GO:0035304	BP	GO:0035304	regulation of protein dephosphorylation	January 10, 2023	90/18723	0.047053711	0.047053711	0.076245898	CALM3	1
GO:0051983	BP	GO:0051983	regulation of chromosome segregation	January 10, 2023	91/18723	0.04756514	0.04756514	0.076245898	IK	1
GO:0032465	BP	GO:0032465	regulation of cytokinesis	January 10, 2023	92/18723	0.048076323	0.048076323	0.076245898	CALM3	1
GO:0007589	BP	GO:0007589	body fluid secretion	January 10, 2023	93/18723	0.048587258	0.048587258	0.076245898	CYBA	1
GO:0032755	BP	GO:0032755	positive regulation of interleukin-6 production	January 10, 2023	93/18723	0.048587258	0.048587258	0.076245898	CYBA	1
GO:1901019	BP	GO:1901019	regulation of calcium ion transmembrane transporter activity	January 10, 2023	93/18723	0.048587258	0.048587258	0.076245898	CALM3	1

(*continued on next page*)

Table 3 (*continued*)

	ONTOLOGY	ID	Description	GeneRatio	BgRatio	pvalue	p.adjust	qvalue	geneID	Count
GO:0006942	BP	GO:0006942	regulation of striated muscle contraction	January 10, 2023	95/ 18723	0.049608388	0.049608388	0.076245898	CALM3	1
GO:0050764	BP	GO:0050764	regulation of phagocytosis	January 10, 2023	95/ 18723	0.049608388	0.049608388	0.076245898	CYBA	1
GO:0070821	CC	GO:0070821	tertiary granule membrane	February 11, 2023	73/ 19550	0.000740084	0.000740084	0.022002043	VAMP1/CYBA	2
GO:0035579	CC	GO:0035579	specific granule membrane	February 11, 2023	91/ 19550	0.001146858	0.001146858	0.022002043	VAMP1/CYBA	2
GO:0030672	CC	GO:0030672	synaptic vesicle membrane	February 11, 2023	109/ 19550	0.001639368	0.001639368	0.022002043	VAMP1/ CALM3	2
GO:0099501	CC	GO:0099501	exocytic vesicle membrane	February 11, 2023	109/ 19550	0.001639368	0.001639368	0.022002043	VAMP1/ CALM3	2
GO:0042581	CC	GO:0042581	specific granule	February 11, 2023	160/ 19550	0.003487741	0.003487741	0.030114678	VAMP1/CYBA	2
GO:0070820	CC	GO:0070820	tertiary granule	February 11, 2023	164/ 19550	0.003660373	0.003660373	0.030114678	VAMP1/CYBA	2
GO:0000922	CC	GO:0000922	spindle pole	February 11, 2023	170/ 19550	0.003926718	0.003926718	0.030114678	IK/CALM3	2
GO:0008021	CC	GO:0008021	synaptic vesicle	February 11, 2023	206/ 19550	0.005708423	0.005708423	0.036001251	VAMP1/ CALM3	2
GO:0030658	CC	GO:0030658	transport vesicle membrane	February 11, 2023	212/ 19550	0.006035504	0.006035504	0.036001251	VAMP1/ CALM3	2
GO:0070382	CC	GO:0070382	exocytic vesicle	February 11, 2023	224/ 19550	0.006715038	0.006715038	0.036049152	VAMP1/ CALM3	2
GO:0030667	CC	GO:0030667	secretory granule membrane	February 11, 2023	311/ 19550	0.012618897	0.012618897	0.061585047	VAMP1/CYBA	2
GO:0005819	CC	GO:0005819	spindle	February 11, 2023	391/ 19550	0.019475078	0.019475078	0.072095003	IK/CALM3	2
GO:0030285	CC	GO:0030285	integral component of synaptic vesicle membrane	January 11, 2023	35/ 19550	0.019522706	0.019522706	0.072095003	VAMP1	1
GO:0097431	CC	GO:0097431	mitotic spindle pole	January 11, 2023	36/ 19550	0.020075371	0.020075371	0.072095003	IK	1
GO:0016607	CC	GO:0016607	nuclear speck	February 11, 2023	412/ 19550	0.021487138	0.021487138	0.072095003	IK/CD2BP2	2
GO:0030133	CC	GO:0030133	transport vesicle	February 11, 2023	412/ 19550	0.021487138	0.021487138	0.072095003	VAMP1/ CALM3	2
GO:0098563	CC	GO:0098563	intrinsic component of synaptic vesicle membrane	January 11, 2023	47/ 19550	0.026136018	0.026136018	0.072643076	VAMP1	1
GO:0031201	CC	GO:0031201	SNARE complex	January 11, 2023	48/ 19550	0.026685293	0.026685293	0.072643076	VAMP1	1
GO:0043209	CC	GO:0043209	myelin sheath	January 11, 2023	48/ 19550	0.026685293	0.026685293	0.072643076	CALM3	1
GO:0071005	CC	GO:0071005	U2-type precatalytic spliceosome	January 11, 2023	50/ 19550	0.027782997	0.027782997	0.072643076	IK	1
GO:0071011	CC	GO:0071011	precatalytic spliceosome	January 11, 2023	53/ 19550	0.029427444	0.029427444	0.072643076	IK	1
GO:0000502	CC	GO:0000502	proteasome complex	January 11, 2023	60/ 19550	0.033254657	0.033254657	0.072643076	PSMD6	1
GO:0005637	CC	GO:0005637	nuclear inner membrane	January 11, 2023	61/ 19550	0.033800281	0.033800281	0.072643076	IFFO1	1

(*continued on next page*)

Table 3 (*continued*)

	ONTOLOGY	ID	Description	GeneRatio	BgRatio	pvalue	p.adjust	qvalue	geneID	Count
GO:0034704	CC	GO:0034704	calcium channel complex	January 11, 2023	65/19550	0.035979976	0.035979976	0.072643076	CALM3	1
GO:1905369	CC	GO:1905369	endopeptidase complex	January 11, 2023	66/19550	0.0365242	0.0365242	0.072643076	PSMD6	1
GO:0001725	CC	GO:0001725	stress fiber	January 11, 2023	71/19550	0.039241137	0.039241137	0.072643076	CYBA	1
GO:0097517	CC	GO:0097517	contractile actin filament bundle	January 11, 2023	71/19550	0.039241137	0.039241137	0.072643076	CYBA	1
GO:0005876	CC	GO:0005876	spindle microtubule	January 11, 2023	72/19550	0.039783688	0.039783688	0.072643076	CALM3	1
GO:0035861	CC	GO:0035861	site of double-strand break	January 11, 2023	73/19550	0.04032596	0.04032596	0.072643076	IFFO1	1
GO:0030670	CC	GO:0030670	phagocytic vesicle membrane	January 11, 2023	76/19550	0.041951107	0.041951107	0.072643076	CYBA	1
GO:0008076	CC	GO:0008076	voltage-gated potassium channel complex	January 11, 2023	79/19550	0.043573752	0.043573752	0.072643076	CALM3	1
GO:0032432	CC	GO:0032432	actin filament bundle	January 11, 2023	80/19550	0.044114078	0.044114078	0.072643076	CYBA	1
GO:0042641	CC	GO:0042641	actomyosin	January 11, 2023	81/19550	0.044654126	0.044654126	0.072643076	CYBA	1
GO:0034705	CC	GO:0034705	potassium channel complex	January 11, 2023	89/19550	0.048964539	0.048964539	0.073631237	CALM3	1
GO:0097525	CC	GO:0097525	spliceosomal snRNP complex	January 11, 2023	90/19550	0.049502096	0.049502096	0.073631237	CD2BP2	1
GO:0043548	MF	GO:0043548	phosphatidylinositol 3-kinase binding	January 11, 2023	34/18368	0.020179534	0.020179534	0.08718129	CALM3	1
GO:0052866	MF	GO:0052866	phosphatidylinositol phosphate phosphatase activity	January 11, 2023	34/18368	0.020179534	0.020179534	0.08718129	FIG4	1
GO:0005484	MF	GO:0005484	SNAP receptor activity	January 11, 2023	36/18368	0.021354955	0.021354955	0.08718129	VAMP1	1
GO:0097718	MF	GO:0097718	disordered domain specific binding	January 11, 2023	36/18368	0.021354955	0.021354955	0.08718129	CALM3	1
GO:0035254	MF	GO:0035254	glutamate receptor binding	January 11, 2023	47/18368	0.027796889	0.027796889	0.08718129	CALM3	1
GO:0043539	MF	GO:0043539	protein serine/threonine kinase activator activity	January 11, 2023	49/18368	0.028963999	0.028963999	0.08718129	CALM3	1
GO:0050661	MF	GO:0050661	NADP binding	January 11, 2023	53/18368	0.0312944	0.0312944	0.08718129	DECR1	1
GO:0016627	MF	GO:0016627	oxidoreductase activity, acting on the CH–CH group of donors	January 11, 2023	60/18368	0.03536037	0.03536037	0.08718129	DECR1	1
GO:0019905	MF	GO:0019905	syntaxin binding	January 11, 2023	74/18368	0.043445802	0.043445802	0.08718129	VAMP1	1

Table 4
KEGG pathways of common gene for COVID-19 and PTB.

	ID	Description	GeneRatio	BgRatio	pvalue	p.adjust	qvalue	geneID	Count
hsa05022	hsa05022	Pathways of neurodegeneration - multiple diseases	March 05, 2023	476/8163	0.0018036005387385	0.0018036005387385	0.0586016813474965	9861/9896/808	3
hsa05418	hsa05418	Fluid shear stress and atherosclerosis	February 05, 2023	139/8163	0.00278357986400608	0.00278357986400608	0.0586016813474965	1535/808	2
hsa05417	hsa05417	Lipid and atherosclerosis	February 05, 2023	215/8163	0.00655217343505484	0.00655217343505484	0.0877739065601638	1535/808	2
hsa05012	hsa05012	Parkinson disease	February 05, 2023	266/8163	0.00991179663506703	0.00991179663506703	0.0877739065601638	9861/808	2
hsa05020	hsa05020	Prion disease	February 05, 2023	273/8163	0.0104231514040194	0.0104231514040194	0.0877739065601638	9861/1535	2
hsa04744	hsa04744	Phototransduction	January 05, 2023	29/8163	0.0176416062661774	0.0176416062661774	0.0939373373474833	808	1
hsa05014	hsa05014	Amyotrophic lateral sclerosis	February 05, 2023	364/8163	0.0181300973594888	0.0181300973594888	0.0939373373474833	9861/9896	2
hsa04130	hsa04130	SNARE interactions in vesicular transport	January 05, 2023	33/8163	0.020055262159076	0.020055262159076	0.0939373373474833	6843	1
hsa05010	hsa05010	Alzheimer disease	February 05, 2023	384/8163	0.0200791058580246	0.0200791058580246	0.0939373373474833	9861/808	2
hsa03050	hsa03050	Proteasome	January 05, 2023	46/8163	0.0278668987520994	0.0278668987520994	0.0944716383403926	9861	1
hsa04720	hsa04720	Long-term potentiation	January 05, 2023	67/8163	0.0403803984330755	0.0403803984330755	0.0944716383403926	808	1
hsa04924	hsa04924	Renin secretion	January 05, 2023	69/8163	0.0415654064766823	0.0415654064766823	0.0944716383403926	808	1
hsa05031	hsa05031	Amphetamine addiction	January 05, 2023	69/8163	0.0415654064766823	0.0415654064766823	0.0944716383403926	808	1
hsa00562	hsa00562	Inositol phosphate metabolism	January 05, 2023	73/8163	0.0439319105624604	0.0439319105624604	0.0944716383403926	9896	1
hsa05214	hsa05214	Glioma	January 05, 2023	75/8163	0.0451134083402389	0.0451134083402389	0.0944716383403926	808	1
hsa04971	hsa04971	Gastric acid secretion	January 05, 2023	76/8163	0.0457037190423035	0.0457037190423035	0.0944716383403926	808	1
hsa05133	hsa05133	Pertussis	January 05, 2023	76/8163	0.0457037190423035	0.0457037190423035	0.0944716383403926	808	1
hsa05140	hsa05140	Leishmaniasis	January 05, 2023	77/8163	0.0462937377643006	0.0462937377643006	0.0944716383403926	1535	1
hsa04970	hsa04970	Salivary secretion	January 05, 2023	92/8163	0.0551090545854003	0.0551090545854003	0.0944716383403926	808	1
hsa04912	hsa04912	GnRH signaling pathway	January 05, 2023	93/8163	0.0556944163407062	0.0556944163407062	0.0944716383403926	808	1
hsa04070	hsa04070	Phosphatidylinositol signaling system	January 05, 2023	97/8163	0.0580329630191848	0.0580329630191848	0.0944716383403926	808	1
hsa04713	hsa04713	Circadian entrainment	January 05, 2023	97/8163	0.0580329630191848	0.0580329630191848	0.0944716383403926	808	1
hsa04750	hsa04750	Inflammatory mediator regulation of TRP channels	January 05, 2023	98/8163	0.058616875142282	0.058616875142282	0.0944716383403926	808	1
hsa04925	hsa04925	Aldosterone synthesis and secretion	January 05, 2023	98/8163	0.058616875142282	0.058616875142282	0.0944716383403926	808	1
hsa04916	hsa04916	Melanogenesis	January 05, 2023	101/8163	0.0603668743242834	0.0603668743242834	0.0944716383403926	808	1
hsa04625	hsa04625	C-type lectin receptor signaling pathway	January 05, 2023	104/8163	0.0621142699870301	0.0621142699870301	0.0944716383403926	808	1
hsa04922	hsa04922	Glucagon signaling pathway	January 05, 2023	107/8163	0.0638590650365957	0.0638590650365957	0.0944716383403926	808	1
hsa04670	hsa04670	Leukocyte transendothelial migration	January 05, 2023	114/8163	0.0679201562979163	0.0679201562979163	0.0944716383403926	1535	1
hsa04722	hsa04722	Neurotrophin signaling pathway	January 05, 2023	119/8163	0.0708122971488159	0.0708122971488159	0.0944716383403926	808	1
hsa04380	hsa04380	Osteoclast differentiation	January 05, 2023	128/8163	0.0760000568705573	0.0760000568705573	0.0944716383403926	1535	1
hsa04114	hsa04114	Oocyte meiosis	January 05, 2023	131/8163	0.0777241513738882	0.0777241513738882	0.0944716383403926	808	1
hsa04728	hsa04728	Dopaminergic synapse	January 05, 2023	132/8163	0.0782982772756722	0.0782982772756722	0.0944716383403926	808	1

(*continued on next page*)

Table 4 (*continued*)

	ID	Description	GeneRatio	BgRatio	pvalue	p.adjust	qvalue	geneID	Count
hsa04270	hsa04270	Vascular smooth muscle contraction	January 05, 2023	134/8163	0.0794456713214461	0.0794456713214461	0.0944716383403926	808	1
hsa04910	hsa04910	Insulin signaling pathway	January 05, 2023	137/8163	0.081164619597707	0.081164619597707	0.0944716383403926	808	1
hsa04915	hsa04915	Estrogen signaling pathway	January 05, 2023	138/8163	0.0817370313721911	0.0817370313721911	0.0944716383403926	808	1
hsa04371	hsa04371	Apelin signaling pathway	January 05, 2023	139/8163	0.0823091578323955	0.0823091578323955	0.0944716383403926	808	1
hsa05017	hsa05017	Spinocerebellar ataxia	January 05, 2023	143/8163	0.0845948126634695	0.0845948126634695	0.0944716383403926	9861	1
hsa04261	hsa04261	Adrenergic signaling in cardiomyocytes	January 05, 2023	150/8163	0.088583748641577	0.088583748641577	0.0944716383403926	808	1
hsa04145	hsa04145	Phagosome	January 05, 2023	152/8163	0.089720886715413	0.089720886715413	0.0944716383403926	1535	1
hsa04921	hsa04921	Oxytocin signaling pathway	January 05, 2023	154/8163	0.0908568894961063	0.0908568894961063	0.0944716383403926	808	1
hsa04218	hsa04218	Cellular senescence	January 05, 2023	156/8163	0.0919917578339573	0.0919917578339573	0.0944716383403926	808	1
hsa04022	hsa04022	cGMP-PKG signaling pathway	January 05, 2023	167/8163	0.0982132934838283	0.0982132934838283	0.098459442089051	808	1
hsa05152	hsa05152	Tuberculosis	January 05, 2023	180/8163	0.105522000276567	0.105522000276567	0.101536250758625	808	1
hsa04621	hsa04621	NOD-like receptor signaling pathway	January 05, 2023	184/8163	0.107761273223756	0.107761273223756	0.101536250758625	1535	1
hsa05034	hsa05034	Alcoholism	January 05, 2023	187/8163	0.109437782999319	0.109437782999319	0.101536250758625	808	1
hsa04613	hsa04613	Neutrophil extracellular trap formation	January 05, 2023	190/8163	0.111111771708027	0.111111771708027	0.101536250758625	1535	1
hsa05167	hsa05167	Kaposi sarcoma-associated herpesvirus infection	January 05, 2023	194/8163	0.113339839909315	0.113339839909315	0.101536250758625	808	1
hsa05169	hsa05169	Epstein-Barr virus infection	January 05, 2023	202/8163	0.117782572729744	0.117782572729744	0.101685636774425	9861	1
hsa05415	hsa05415	Diabetic cardiomyopathy	January 05, 2023	203/8163	0.118336659796237	0.118336659796237	0.101685636774425	1535	1
hsa04015	hsa04015	Rap1 signaling pathway	January 05, 2023	210/8163	0.122207478937182	0.122207478937182	0.1017203248805	808	1
hsa05170	hsa05170	Human immunodeficiency virus 1 infection	January 05, 2023	212/8163	0.123310926376257	0.123310926376257	0.1017203248805	808	1
hsa04024	hsa04024	cAMP signaling pathway	January 05, 2023	221/8163	0.128262716081975	0.128262716081975	0.1017203248805	808	1
hsa05208	hsa05208	Chemical carcinogenesis - reactive oxygen species	January 05, 2023	223/8163	0.12936006905401	0.12936006905401	0.1017203248805	1535	1
hsa05163	hsa05163	Human cytomegalovirus infection	January 05, 2023	225/8163	0.130456316659241	0.130456316659241	0.1017203248805	808	1

(*continued on next page*)

Table 4 (*continued*)

	ID	Description	GeneRatio	BgRatio	pvalue	p.adjust	qvalue	geneID	Count
hsa04014	hsa04014	Ras signaling pathway	January 05, 2023	235/8163	0.135921003403764	0.135921003403764	0.104054356672738	808	1
hsa04020	hsa04020	Calcium signaling pathway	January 05, 2023	240/8163	0.138643024374669	0.138643024374669	0.104242875469676	808	1
hsa05016	hsa05016	Huntington disease	January 05, 2023	306/8163	0.173935317041476	0.173935317041476	0.128484075376898	9861	1
hsa04740	hsa04740	Olfactory transduction	January 05, 2023	439/8163	0.241541027528449	0.241541027528449	0.175347388405407	808	1

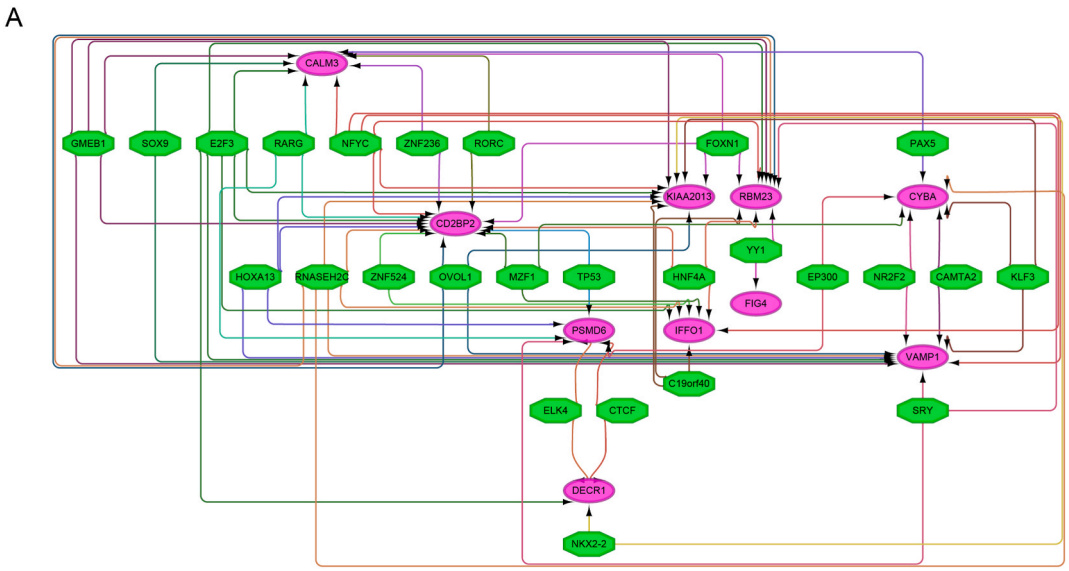

Fig. 6. The transcriptional regulatory network. Red and green represent upregulated and downregulated genes, respectively. Oval and polygon symbols represent transcription factors and target genes, respectively.

established approach for converting gene expression data into co-expression modules to thereby facilitate the elucidation of critical biological processes and essential genes. Using this approach, we identified two modules consisting of co-expressed genes associated with COVID-19 and PTB disease states. Through meticulous bioinformatics analysis of genes within these modules, we identified key genes and pathways pivotal in the development and progression of both diseases.

In addition, real-time qPCR analysis of blood samples obtained from COVID-19 and TB patients revealed upregulated expression of almost all of these common genes, thus suggesting these genes may serve as targets of potential drug treatments for these infectious diseases. Subsequent analysis of drug interactions with these common genes enabled the prediction of drug candidates for the treatment of individuals afflicted with both diseases. Nonetheless, additional experiments and clinical trials are needed to validate potential drug treatments for PTB and COVID-19 identified in this study with regard to biological functions, therapeutic effects, and safety.

6. Conclusions

The results of this study furnish experimentally validated, bioinformatics-supported evidence establishing a potential link between the pathogenesis of PTB and COVID-19. Through a comprehensive WGCNA analysis and rigorous experiments, we identified 10 common genes that play pivotal roles in the pathogenic mechanisms of both COVID-19 and TB. Notably, these genes are significantly enriched in functions related to critical biological processes, including RNA splicing and extracellular vesicles, underscoring their central roles in processes relevant to both diseases.

Our analysis of the regulatory network, comprised of the aforementioned common genes and predicted interacting TFs, significantly enriched our understanding of gene regulation, biological processes, and pathogenic mechanisms underlying comorbid PTB and COVID-19. Additionally, an examination of drugs within the DSigDB database that may interact with these common genes unveiled potential drug molecules and drug-target interactions. This information guides the development of early diagnostic methods and novel therapeutic strategies for treating patients afflicted with both diseases. In this study, we observed common transcriptional changes only in macrophages derived from human blood. To elucidate the mechanistic crosstalk of these common genes in the context of tuberculosis and COVID-19, future research may involve a more in-depth investigation in animal models. This will further enhance our understanding of the shared pathogenic mechanisms associated with these common genes.

Data availability

Upon reasonable request, the corresponding author will provide access to the datasets generated or analyzed during the current study.

Funding

This work was supported by the Beijing Hospitals Authority Clinical Medicine Development of Special Funding (ZYLX202122).

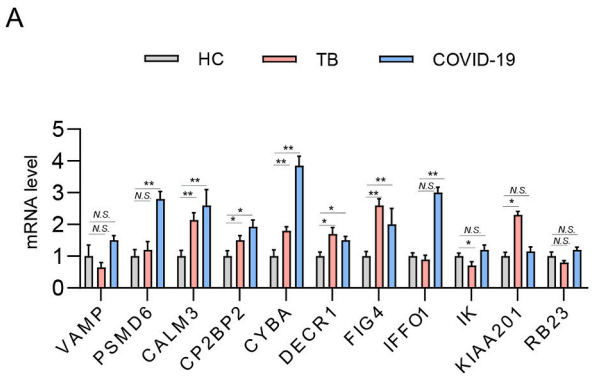

Fig. 7. Common genes validation. mRNA levels of common genes related to both COVID-19 and PTB were analyzed using semi-quantitative PCR. *p < 0.05, **p < 0.01.

CRediT authorship contribution statement

Xin Liu: Writing – original draft, Project administration, Formal analysis. **Haoran Li:** Project administration, Formal analysis. **Yilin Wang:** Writing – review & editing, Writing – original draft. **Shanshan Li:** Writing – review & editing, Methodology. **Weicong Ren:** Writing – review & editing, Methodology. **Jinfeng Yuan:** Writing – review & editing, Conceptualization. **Yu Pang:** Writing – review & editing, Funding acquisition, Conceptualization.

Declaration of competing interest

The authors declare that they have no known competing financial interests or personal relationships that could have appeared to influence the work reported in this paper.

Appendix A. Supplementary data

Supplementary data to this article can be found online at https://doi.org/10.1016/j.heliyon.2024.e28664.

References

[1] J. Chakaya, et al., The WHO Global Tuberculosis 2021 Report - not so good news and turning the tide back to End TB, Int. J. Infect. Dis. 124 (Suppl 1) (2022) S26–s29.
[2] C.R. Horsburgh Jr., Priorities for the treatment of latent tuberculosis infection in the United States, N. Engl. J. Med. 350 (20) (2004) 2060–2067.
[3] P.J. Dodd, et al., The impact of HIV and antiretroviral therapy on TB risk in children: a systematic review and meta-analysis, Thorax 72 (6) (2017) 559–575.
[4] S.Y. Rodriguez-Takeuchi, M.E. Renjifo, F.J. Medina, Extrapulmonary tuberculosis: Pathophysiology and Imaging findings, Radiographics 39 (7) (2019) 2023–2037.
[5] M.M. Looney, et al., *Conference report: WHO Meeting Report on mRNA-Based Tuberculosis Vaccine Development.* Vaccine, 2023.
[6] C. Huang, et al., 6-month consequences of COVID-19 in patients discharged from hospital: a cohort study, Lancet 397 (10270) (2021) 220–232.
[7] C.G.K. Ziegler, et al., Impaired local intrinsic immunity to SARS-CoV-2 infection in severe COVID-19, Cell 184 (18) (2021) 4713–4733.e22.
[8] I.H. Elrobaa, K.J. New, COVID-19: pulmonary and extra pulmonary manifestations, Front. Public Health 9 (2021) 711616.
[9] K. Sreenath, et al., Coinfections with other respiratory pathogens among patients with COVID-19, Microbiol. Spectr. 9 (1) (2021) e0016321.
[10] E. Sharifipour, et al., Evaluation of bacterial co-infections of the respiratory tract in COVID-19 patients admitted to ICU, BMC Infect. Dis. 20 (1) (2020) 646.
[11] M. Tadolini, et al., On tuberculosis and COVID-19 co-infection, Eur. Respir. J. 56 (2) (2020).
[12] Tuberculosis and COVID-19 co-infection: description of the global cohort, Eur. Respir. J. 59 (3) (2022).
[13] J. Piñero, et al., DisGeNET: a comprehensive platform integrating information on human disease-associated genes and variants, Nucleic Acids Res. 45 (D1) (2017) D833–d839.
[14] D. Sheerin, et al., Immunopathogenic overlap between COVID-19 and tuberculosis identified from transcriptomic meta-analysis and human macrophage infection, iScience 25 (6) (2022) 104464.
[15] A.K. Banerjee, et al., SARS-CoV-2 disrupts splicing, translation, and protein trafficking to suppress host defenses, Cell 183 (5) (2020) 1325–1339.e21.
[16] D.R.A. Sanya, C. Cava, D. Onésime, Roles of RNA-binding proteins in neurological disorders, COVID-19, and cancer, Hum. Cell 36 (2) (2023) 493–514.
[17] A. Singh, et al., The SARS-CoV-2 UTR's intrudes host RBP's and modulates cellular splicing, Adv Virol 2023 (2023) 2995443.
[18] M. Lyu, et al., From tuberculosis bedside to bench: UBE2B splicing as a potential biomarker and its regulatory mechanism, Signal Transduct. Targeted Ther. 8 (1) (2023) 82.
[19] W. Zhang, et al., Mycobacterium tuberculosis H37Rv infection regulates alternative splicing in Macrophages, Bioengineered 9 (1) (2018) 203–208.
[20] J. Crow, G. Samuel, A.K. Godwin, Beyond tumor mutational burden: potential and limitations in using exosomes to predict response to immunotherapy, Expert Rev. Mol. Diagn 19 (12) (2019) 1079–1088.
[21] P. Su, et al., A review of extracellular vesicles in COVID-19 diagnosis, treatment, and prevention, Adv. Sci. (2023) e2206095.
[22] M.A. Ellul, et al., Neurological associations of COVID-19, Lancet Neurol. 19 (9) (2020) 767–783.
[23] R.J. Wilkinson, et al., Tuberculous meningitis, Nat. Rev. Neurol. 13 (10) (2017) 581–598.
[24] Q. Ye, et al., Clinical analysis of 103 cases of tuberculous meningitis complicated with hyponatremia in adults, Neurol. Sci. 43 (3) (2022) 1947–1953.

[25] C. Chen, et al., Single-cell analysis of adult human heart across healthy and cardiovascular disease patients reveals the cellular landscape underlying SARS-CoV-2 invasion of myocardial tissue through ACE2, J. Transl. Med. 21 (1) (2023) 358.
[26] C. Freund, et al., Dynamic interaction of CD2 with the GYF and the SH3 domain of compartmentalized effector molecules, EMBO J. 21 (22) (2002) 5985–5995.
[27] H. Zhou, et al., DECR1 directly activates HSL to promote lipolysis in cervical cancer cells, Biochim. Biophys. Acta Mol. Cell Biol. Lipids 1867 (3) (2022) 159090.
[28] G.Y. Lee, S.N. Han, The role of vitamin E in immunity, Nutrients 10 (11) (2018).
[29] S.N. Han, et al., Vitamin E supplementation increases T helper 1 cytokine production in old mice infected with influenza virus, Immunology 100 (4) (2000) 487–493.
[30] Q. Su, et al., Trichostatin A ameliorates Alzheimer's disease-related pathology and cognitive deficits by increasing albumin expression and Aβ clearance in APP/PS1 mice, Alzheimer's Res. Ther. 13 (1) (2021) 7.
[31] L. Zhang, et al., The protection of selenium against cadmium-induced mitophagy via modulating nuclear xenobiotic receptors response and oxidative stress in the liver of rabbits, Environ. Pollut. 285 (2021) 117301.
[32] Z. Huang, A.H. Rose, P.R. Hoffmann, The role of selenium in inflammation and immunity: from molecular mechanisms to therapeutic opportunities, Antioxidants Redox Signal. 16 (7) (2012) 705–743.
[33] M. Vinceti, et al., Selenium for preventing cancer, Cochrane Database Syst. Rev. 1 (1) (2018) Cd005195.
[34] A.L. Maricuto, et al., Amoebic liver abscess in a COVID-19 patient: a case report, BMC Infect. Dis. 21 (1) (2021) 1134.
[35] A. Roczkowsky, et al., COVID-19 induces neuroinflammation and suppresses peroxisomes in the brain, Ann. Neurol. (2023).
[36] A. Behera, et al., Mycobacterium tuberculosis acetyltransferase suppresses oxidative stress by inducing peroxisome formation in macrophages, Int. J. Mol. Sci. 23 (5) (2022).